The nuclear magnetic shielding as a function of internuclear separation

Cynthia J. Jameson and Angel C. de Dios
Department of Chemistry, University of Illinois at Chicago, Chicago, Illinois 60680

(Received 28 September 1992; accepted 22 October 1992)

Ab initio calculations of nuclear magnetic shielding surfaces for ^{23}Na in the NaH molecule, ^{39}Ar in ArNe, ^{21}Ne in NeHe, and ^{39}Ar in Ar···NaH are carried out over a wide range of internuclear separations, using a local origin method (LORG) which damps out the long-range errors due to incomplete basis sets. The R dependence of the intermolecular shielding in the attractive region of the potential in these systems and in Ar···Ar and Ar···Na^+ are consistent with the long-range limiting forms associated with the shielding hyperpolarizability in conjunction with a mean square electric field approximation. The Cl and F shieldings over the range of nuclear displacements spanning the classical turning points of the ground vibrational states of ClF and F_2 are found to be remarkably superposable upon scaling by the factors $\langle a_0^3/r^3\rangle \cdot R_e$. This holds as well for ClH compared with FH. The shielding of ^{23}Na and ^{7}Li in NaH and LiH molecules are almost superposable. These and the scaling of the intermolecular shielding in rare gas pairs indicate some general similarities of shielding surfaces. The systematic variation in the signs and magnitudes of the first derivative of X nuclear shielding at the equilibrium geometry in XH_n molecules of the first and second row of the Periodic Table are shown to be consistent with a general shape for the shielding function $\sigma(R)$, which we have found in rare gas pairs and for ^{23}Na in NaH.

I. INTRODUCTION

The nuclear magnetic shielding is a function of molecular geometry. The mathematical surface which describes the nuclear shielding in terms of various parameters of molecular geometry, such as internuclear separations, is itself not directly observed in experiments. However, it reveals itself in several observables such as the density coefficient of the NMR (nuclear magnetic resonance) chemical shift in gases, the temperature dependence of the chemical shift in the vibrating rotating nearly isolated molecule, and the mass dependence of the chemical shift (the so-called isotope shifts).[1,2] In condensed phases there are gas-to-liquid shifts or solvent shifts, matrix-induced chemical shifts, site-dependent shielding tensors in crystalline solids, and adsorption shifts in adsorbed species. In the interpretation of these various data, the problem can be viewed in two parts which are intimately connected: First is the shielding surface itself for the system in question: second is the appropriate sampling of this shielding surface during dynamic processes such as collisions in the gas phase, rovibrational motion, site-to-site hopping, or fast exchange in physisorbed phases.

Some intramolecular shielding functions have been investigated in the immediate vicinity of the equilibrium geometry of small molecules,[3–10] revealing first and second derivatives with respect to displacements from equilibrium nuclear positions. However, apart from the ^{1}H shielding in the H_2^+ molecule,[11] only the ^{15}N shielding as a function of the inversion coordinate in the NH_3 molecule has been calculated for a wide range of values of the coordinate.[9]

In this paper we will consider the shielding surface for various two-atom systems, the simplest cases in that they involve only one geometrical parameter, the internuclear separation. We examine their similarities and differences, with the goal of gaining some insight into the general features, if any, of the shielding as a function of internuclear distance.

II. THE SHAPE OF THE INTRAMOLECULAR SHIELDING FUNCTION IN DIATOMIC MOLECULES

We have determined the form of the intermolecular shielding function for ^{39}Ar in Ar···Ar over a wide range of separations (0.5–7 Å)[12] and noted its similarity to the intramolecular shielding function for ^{1}H in the H_2^+ molecule, which had been calculated accurately from 0 to 22 a.u.[11] From the large positive united atom value, the shielding is seen to decrease until it reaches a minimum which occurs at an internuclear separation much shorter than the r_0 of the potential function. The shielding from this point asymptotically approaches the value for the isolated atom, exhibiting a behavior close to $R^{-6.67}$ at large distances. The close resemblance exhibited by the intermolecular shielding functions for the rare gas atoms (in Figs. 2 and 11 of Ref. 12) to this intramolecular shielding function is truly intriguing. Moreover, the R dependence of the shielding in the H_2^+ molecule at separations longer than the internuclear separation at which the minimum in the shielding function occurs is surprisingly similar to that of the argon dimer system. As shown in Fig. 13 of Ref. 12, the intramolecular shielding function in this region behaves as $R^{-6.0}$. However, ^{1}H shielding is not typical of most nuclei, so we need to investigate heavier nuclei in diatomic molecules. In order to determine the shape of the intramolecular shielding function for a diatomic molecule, it will be necessary to do calculations of $\sigma(R)$ over a wide range of R values. In molecules such as HF or F_2, the derivative of the shielding

 0021-9606/93/032208-10$06.00

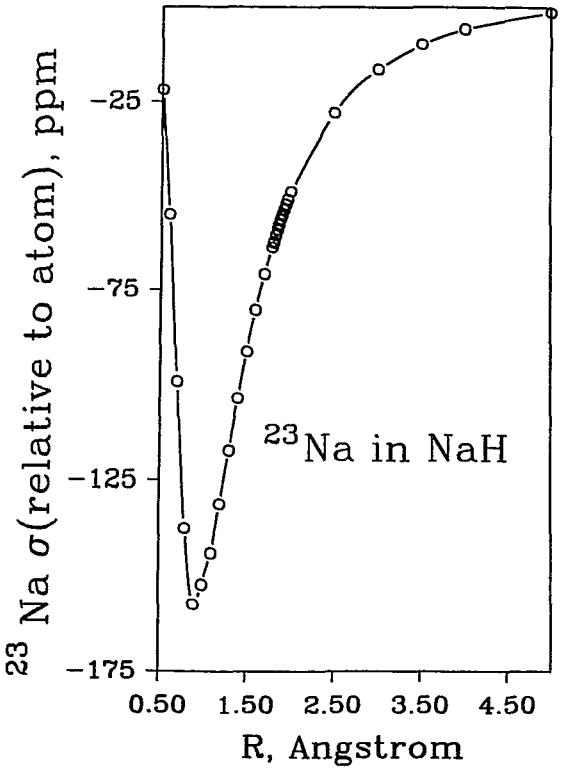

FIG. 1. The ^{23}Na shielding surface for the NaH molecule, calculated using the LORG method.

function at the equilibrium geometry is negative.[10,13] This means that if the shape of the $\sigma(R)$ function is indeed similar to that for ^{39}Ar in Ar_2, the shielding must decrease further, reach a minimum, and start to increase again toward the separated atom values, all in the region of R values greater than the equilibrium separation. Unfortunately, in these molecules, the minimum shielding cannot be observed in the calculations because the separated entities are non-S states of the atoms. At large internuclear separations the orbital paramagnetism of the ground state F atom comes into play, leading to very large negative shielding values and a minimum in the shielding function in not observed. If one is to observe the true shape of $\sigma(R)$ in a diatomic molecule, it will have to be in those systems which dissociate into S-state atoms and/or in which the derivative of the shielding is *positive* at the equilibrium geometry. One can then investigate R values shorter than the equilibrium separation and there should be no problem in doing this, unless, of course, the minimum shielding occurs at distances so short that avoided crossings with higher energy potential surfaces complicate the picture. Diatomic molecules that are known to have positive shielding derivatives at R_e, and are therefore likely candidates, are NaH and LiH. The latter has a fairly short R_e and we did not observe any minimum before reaching 0.5 Å. We did obtain the shielding function of ^{23}Na in NaH, shown in Fig. 1. We see that the shape is indeed similar to that for ^{39}Ar shielding in Ar_2 and for ^{1}H shielding in H_2^+ molecule.

For the calculation of the intermolecular shielding, it is even more important to damp out the errors which result from incomplete cancellation of large positive and negative long-range contributions. In calculations of magnetic properties, this is known as a gauge origin problem. For these reasons, we have chosen a local origin method that effectively damps out the errors in calculating the long-range contributions to the diamagnetic and paramagnetic terms and which can be extended to include second-order correlation contributions. The localized orbital local origin (LORG) method developed by Hansen and Bouman[14] and second order LORG (SOLO)[15] were used in this work. In previous calculations using LORG[8,9] we have found that basis sets for atoms in the second row of the Periodic Table should include a standard triple zeta plus three d polarization functions in order to achieve acceptable accuracy. Therefore, for this paper, we have used a 6–311G basis plus three d polarization functions. GAUSSIAN 88[16] provided the SCF results which served as input to the LORG calculations using RPAC 8.5.[17] All results presented in this paper were obtained using LORG, except for the previously reported SOLO calculations on Ar_2 and ArNa.$^+$[12]

III. THE EFFECTS OF CHARGE ON SHIELDING, THE LONG-RANGE LIMIT

Whereas we have shown that the shielding for ^{39}Ar in Ar_2 behaves as approximately $R^{-6.67}$ at intermediate internuclear separations (in the range of R values 2 to 4 Å), and the ^{1}H shielding in H_2^+ molecule has a $R^{-6.0}$ behavior at large separations (7 to 22 a.u.), there is a somewhat different behavior, which we attribute to the contributions of induction to the shielding, when electrical charges are involved. For example, let us compare ^{39}Ar shielding in Ar···Ne with that in the isoelectronic Ar···Na$^+$ in Fig. 2. The ArNa$^+$ results were reported earlier,[12] whereas the ArNe results are from this work. From a plot of $\log[\sigma(\infty)-\sigma(R)]$/ppm vs $\log(R/\text{Å})$, we find that the approach of $\sigma(R)$ to the separated atoms value is approximately $R^{-3.44}$ for ^{39}Ar in ArNa$^+$ in the range $R=1.5$ to 5 Å, whereas it is (typical for rare gas pairs) approximately $R^{-6.79}$ for ^{39}Ar in ArNe (in the range $R=2$ to 4 Å). An understanding of the differences in the R dependence can be gained from the expected functional forms of $\sigma(R)$ in the long-range limit.

The long-range limiting behavior in these systems can be modeled by considering the effects of the neighboring atom or ion on the ^{39}Ar shielding in terms of the electric fields F_γ created by the neighbor at the position of the ^{39}Ar nucleus. The shielding of a nucleus in the presence of an electric field is given by[18–20]

$$\sigma_{\alpha\alpha}=\sigma_{\alpha\alpha}^{(0)}+\left(\frac{\partial\sigma_{\alpha\alpha}}{\partial F_\gamma}\right)_{F_\gamma=0}F_\gamma + \left(\frac{\partial^2\sigma_{\alpha\alpha}}{\partial F_\gamma\partial F_\beta}\right)_{F_\beta=F_\gamma=0}F_\beta F_\gamma+\cdots. \quad (1)$$

We may further include the effects of electric field gradients $F_{\gamma\beta}$,

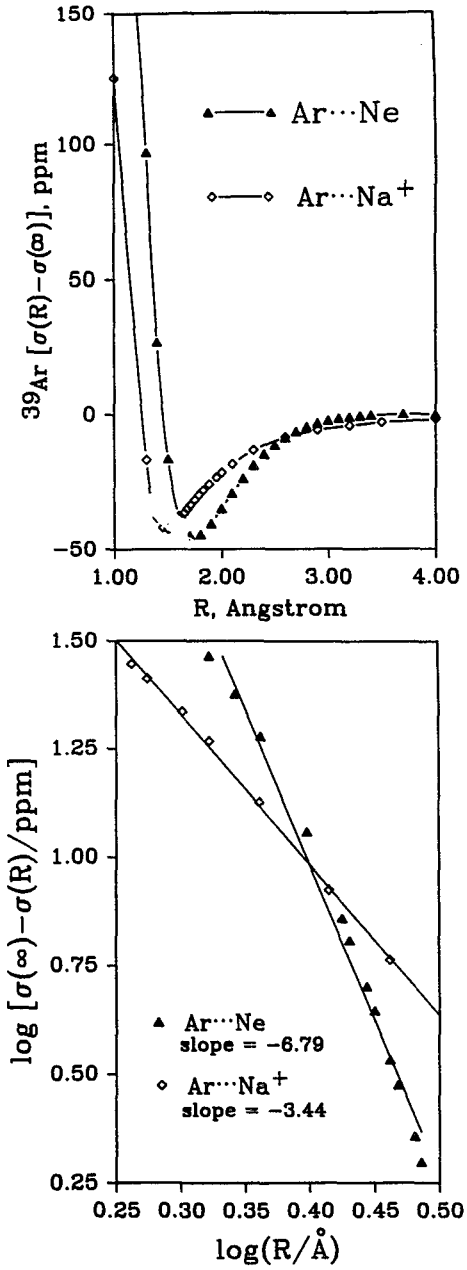

FIG. 2. The *ab initio* ^{39}Ar shielding surfaces $[\sigma(R)-\sigma(\infty)]$ for the isoelectronic systems Ar···Ne and Ar···Na$^+$. The behavior of these functions at intermediate to large R are shown to be close to R^{-6} to R^{-8} and R^{-4}, respectively, consistent with the mean field model [see Eqs. (11) and (15)].

$$\left(\frac{\partial\sigma_{\alpha\alpha}}{\partial F_{\gamma\beta}}\right)_{F_{\gamma\beta}=0} F_{\gamma\beta}+\cdots.$$

For an Ar atom, the first derivatives of shielding with respect to the electric field (the shielding polarizability, a term coined by Dykstra[21,22]) vanish by symmetry,

$$\left(\frac{\partial\sigma_{\alpha\alpha}}{\partial F_{\gamma}}\right)_{F_{\gamma}=0}=0. \tag{2}$$

For an isolated atom there are only two independent second derivatives (shielding hyperpolarizabilities). One corresponds to $B_0\| F$, i.e.,

$$\left(\frac{\partial^2\sigma_{xx}}{\partial F_x^2}\right)_{F_x=0}=\sigma^{(2)}_{xx,x,x}=\sigma^{(2)}_{yy,y,y}=\sigma^{(2)}_{zz,z,z}. \tag{3}$$

The other corresponds to $B_0\perp F$, i.e.,

$$\sigma^{(2)}_{xx,y,y}=\sigma^{(2)}_{yy,z,z}=\sigma^{(2)}_{zz,x,x}=\sigma^{(2)}_{xx,z,z}=\sigma^{(2)}_{zz,y,y}=\sigma^{(2)}_{yy,x,x}. \tag{4}$$

In an external uniform electrical field, the shielding of an atom is given by

(xx component):

$$\sigma_{xx}=\sigma^{(0)}_{xx}+\tfrac{1}{2}\sigma^{(2)}_{xx,x,x}F^2_x+\tfrac{1}{2}\sigma^{(2)}_{xx,y,y}F^2_y+\tfrac{1}{2}\sigma^{(2)}_{xx,z,z}F^2_z+\cdots. \tag{5}$$

There are no cross terms in the electric field components since derivatives of the type $\sigma^{(2)}_{xx,x,z}$ vanish for an atom.

We now consider the situation in which the electric field is due to a neighbor atom, ion, or molecule. **R** being the vector from the origin of the 1 (the NMR nucleus) to 2 (the neighbor), the electric field at point 1 due to a charge at point 2 is given by[23]

$$F_{1\alpha}=-\nabla_\alpha\left(\frac{q_2}{R}\right)=-R_\alpha R^{-3}q_2, \tag{6}$$

and if other electric multipoles are present at point 2, the electric field at 1 is given by,

$$F_{1\alpha}=q_2(-R_\alpha R^{-3})+\mu_{2\beta}(3R_\alpha R_\beta-R^2\delta_{\alpha\beta})R^{-5}$$
$$-\tfrac{1}{3}\theta_{2\beta\gamma}[5R_\alpha R_\beta R_\gamma-R^2(R_\alpha\delta_{\beta\gamma}+R_\beta\delta_{\gamma\alpha}$$
$$+R_\gamma\delta_{\alpha\beta})]R^{-7}+\cdots. \tag{7}$$

Therefore, the long-range limit of the shielding for ^{39}Ar in the presence of Na$^+$, relative to the free Ar atom, is

(xx component):

$$[\sigma_{xx}-\sigma^{(0)}_{xx}]=\tfrac{1}{2}\sigma^{(2)}_{xx,x,x}F^2_x+\tfrac{1}{2}\sigma^{(2)}_{xx,y,y}F^2_y+\tfrac{1}{2}\sigma^{(2)}_{xx,z,z}F^2_z+\cdots, \tag{8}$$

which becomes

$$=\tfrac{1}{2}\sigma^{(2)}_{xx,x,x}q_2^2X^2R^{-6}+\sigma^{(2)}_{xx,z,z}q_2^2(Y^2+Z^2)R^{-6}+\cdots, \tag{9}$$

where X, Y, and Z are the coordinates of position 2 relative to the ^{39}Ar nucleus at the origin of the atom at 1 when the Na$^+$ ion is approximated at long range by a point charge. Similar expressions hold for the yy and the zz components of the ^{39}Ar shielding. If we are observing only the isotropic shielding $\sigma_{\rm iso}$, then the 1–2 pair at a fixed separation R is considered to be tumbling freely in the magnetic field B_0. Therefore, where

$$\sigma_{\rm iso}\equiv\tfrac{1}{3}(\sigma_{xx}+\sigma_{yy}+\sigma_{zz}),$$

we have

$$[\sigma_{\rm iso}-\sigma^{(0)}_{\rm iso}]=\tfrac{1}{3}\left[\tfrac{1}{2}\sigma^{(2)}_{zz,z,z}+\sigma^{(2)}_{zz,x,x}\right]q_2^2R^{-4}+\cdots. \tag{10}$$

For a ^{1}H nucleus in a hydrogen atom at a distance R from a point charge q_2, the quantities in Eq. (10) including all inverse powers from R^{-4} up to the R^{-8} terms have been

calculated exactly by Musher.[24] To Eq. (10) must be added the long-range terms also present even in the absence of a charge or multipole on 2, as for the ^{39}Ar nucleus in the ArNe system;

$$[\sigma_{\rm iso}-\sigma_{\rm iso}^{(0)}]=\tfrac{1}{3}\left[\tfrac{1}{2}\sigma_{zz,z,z}^{(2)}+\sigma_{zz,x,x}^{(2)}\right]\left[-\frac{C_6}{\alpha_{\rm Ar}}R^{-6}-\frac{1}{\alpha_{\rm Ar}}\times\left(C_8-5C_6\frac{C_{\rm Ne}}{\alpha_{\rm Ne}}\right)R^{-8}-\cdots\right]. \quad (11)$$

The two terms inside the square brackets provide the mean square field arising from the quantum mechanical dispersion term, which we had previously approximated by the London formula $\frac{3}{2}\alpha_{\rm Ne}[U_{\rm Ar}U_{\rm Ne}/(U_{\rm Ar}+U_{\rm Ne})]R^{-6}$ in Ref. 12. Here C_6 and C_8 are the coefficients (negative quantities) of the dispersion terms in R^{-6} and R^{-8} for the Ar$\cdots$Ne system. The last term in the square brackets is the mean square field due to the effective mean quadrupole moment, where $C_{\rm Ne}$ is the electric quadrupole polarizability of the atom.[23] The relation of the mean-square field to the dispersion energy of a pair of interacting atoms goes back to the work of London,[25,26] and more recently, Buckingham and Clarke.[27]

What about the electric field gradient term? The derivatives $(\partial\sigma_{\mu\nu}/\partial F_{\alpha\beta})_{F_{\alpha\beta}=0}$ are subject to the same symmetry rules as are the second derivatives with respect to fields $F_\alpha F_\beta$. Thus for ^{39}Ar,

$$\sigma_{xx,xx}^{(1)}=\sigma_{yy,yy}^{(1)}=\sigma_{zz,zz}^{(1)},$$

$$\sigma_{xx,yy}^{(1)}=\sigma_{yy,zz}^{(1)}=\sigma_{zz,xx}^{(1)}=\sigma_{xx,zz}^{(1)}=\sigma_{zz,yy}^{(1)}=\sigma_{yy,xx}^{(1)} \quad (12)$$

and derivatives of the type $\sigma_{xx,xz}^{(1)}$ are zero. The electric field gradient at 1 due to an electric charge at 2 is given by[23]

$$F_{1\alpha\beta}=\nabla_\alpha F_{1\beta}=-q_2(3R_\alpha R_\beta-R^2\delta_{\alpha\beta})R^{-5}. \quad (13)$$

The shielding terms due to the electric field gradient created by the Na^+ ion at the ^{39}Ar nucleus are therefore of the form

$$\sigma_{xx,xx}^{(1)}[-q_2(3X^2-R^2)R^{-5}]+\sigma_{xx,yy}^{(1)}[-q_2(3Y^2+3Z^2-2R^2)R^{-5}]. \quad (14)$$

These contributions to individual tensor elements, as in Eq. (14), were first considered by Buckingham and Lawley.[28] The contribution to the isotropic average shielding is one-third the sum of three terms of this type, which vanishes.

Therefore, the isotropic shielding of ^{39}Ar in Ar$\cdots$Na$^+$ in the long-range limit is

$$[\sigma_{\rm iso}-\sigma_{\rm iso}^{(0)}]_{^{39}{\rm Ar}}=\tfrac{1}{3}\{\tfrac{1}{2}\sigma_{zz,z,z}^{(2)}+\sigma_{zz,x,x}^{(2)}\}_{\rm Ar}\left[q_{\rm Na^+}^2R^{-4}-\frac{C_6}{\alpha_{\rm Ar}}R^{-6}-\frac{1}{\alpha_{\rm Ar}}\left(C_8-5C_6\frac{C_{\rm Na^+}}{\alpha_{\rm Na^+}}\right)R^{-8}-\cdots\right]. \quad (15)$$

We can see the long tail of this function in the R^{-4} term. Not surprisingly, the *ab initio* shielding function for the ^{39}Ar$\cdots$Na$^+$ system has a $R^{-3.44}$ dependence in the range of $R=1.5$ to 5 Å, becoming R^{-4} for the larger R values in this range, whereas the ArNe system has a $R^{-6.79}$ dependence in the range of $R=2$ to 4 Å.

A similar situation holds for the ^{23}Na shielding in the Na^+ ion in the presence of H^- ion in the long range limit. The electric field gradient terms at the ^{23}Na nucleus due to the induced dipole at position 2 (H^- ion) generated by the presence of charge q_1 (Na^+ ion) can be considered, but here too, the sum of the electric field gradient contributions to the three components of shielding vanish. Thus in the long range limit of the separated ions, the same expression given in Eq. (15) holds for the ^{23}Na shielding in $Na^+\cdots H^-$ except that one should replace ^{39}Ar by ^{23}Na and Na^+ by H^-. Furthermore, one should add to Eq. (15) those terms involving the electric field at Na^+ created by the electrical moments induced at H^- by the Na^+ ion. The first nonvanishing term of this type is $\alpha_2^2q_1^2R^{-10}+\cdots$, where the subscripts 1 and 2 refer to Na^+ and H^-, respectively. The shape of the *ab initio* ^{23}Na shielding function in the NaH diatomic molecule does have a long tail, i.e., $R^{-2.64}$ in the vicinity of r_e and up to 3.6 Å, going to R^{-4} at longer range, similar to that for ^{39}Ar in Ar$\cdots$Na$^+$. In the electronic ground state of the NaH molecule, there is some mixing of the ionic Na^+H^- limit even at $R=r_e$.[29] This explains, in part, the similarity of the ^{23}Na shielding function for the NaH molecule with that for ^{39}Ar in $ArNa^+$.

Let us consider ^{39}Ar in Ar$\cdots$NaH (collinear) in order to examine the effect on the shielding of the electric dipole moment of a neighbor molecule. By modifying the length of the NaH bond in this system we have observed the dependence of the shielding on both the magnitude of the dipole moment and the internuclear separation. For ^{39}Ar in Ar$\cdots$NaH (collinear), the long-range limiting behavior due to the dipole moment of NaH can be derived from Eq. (7).

We consider the isotropic tumbling of the collinear system in the magnetic field. Once again, the sum of the contributions to the three components of shielding vanishes for the electric field gradient term. Thus we have, for the collinear Ar$\cdots$NaH system in the long-range limit,[27,30]

$$[\sigma_{\rm iso}-\sigma_{\rm iso}^{(0)}]_{\rm Ar}=\tfrac{1}{3}\{\tfrac{1}{2}\sigma_{zz,z,z}^{(2)}+\sigma_{zz,x,x}^{(2)}\}_{\rm Ar}\cdot\left[4\mu_2^2R^{-6}+\tfrac{9}{2}\theta_2^2R^{-8}+\cdots-\frac{C_6}{\alpha_1}R^{-6}-\frac{1}{\alpha_1}\times\left(C_8-5C_6\frac{C_2}{\alpha_2}\right)R^{-8}-\cdots\right]. \quad (16)$$

The *ab initio* shielding values of ^{39}Ar in the Ar$\cdots$NaH system is shown in Fig. 3 where it is easily seen that the R^{-6} dependence in the range $R_{\rm ArNa}>2.5$ Å is more like that which is found for ^{39}Ar in ArNe than the $R^{-3.44}$ found in $ArNa^+$. By adjusting the Na–H bond length the electric dipole moment of NaH can be tuned. This provides us with the dependence of the *ab initio* shielding of ^{39}Ar on the electric dipole moment. $[\sigma(R)-\sigma(\infty)]$ of ^{39}Ar behaves as expected from the long-range dependence on the square of

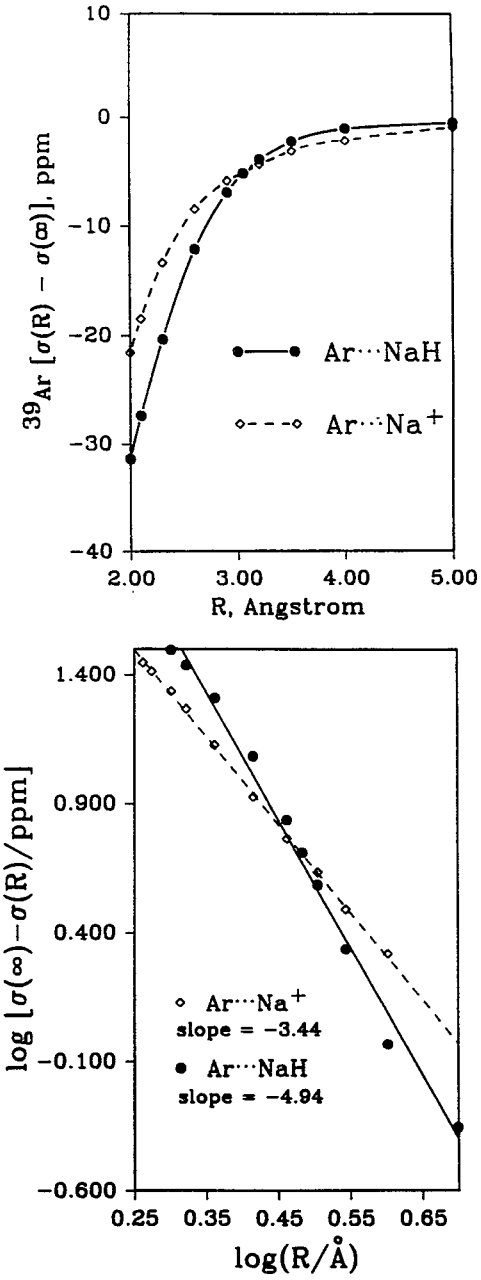

FIG. 3. The *ab initio* ^{39}Ar shielding surfaces Ar···Na$^+$ and Ar···NaH (collinear) show $\sim R^{-4}$ and $\sim R^{-6}$ behavior at large R, as predicted by a mean field model [see Eqs. (15) and (18)].

the dipole moment. At a distance of 5 Å, the intermolecular shielding, $[\sigma(R)-\sigma(\infty)]$ of ^{39}Ar is -0.44 ppm in the Ar···NaH system and only -0.06 ppm in the Ar···Ar system. Clearly the $4\mu^2$ term is dominant at this distance. On the other hand, at shorter distances, as shown in Table I, there is a greater deshielding at the Ar interacting with the NaH molecule having the smaller dipole moment. We also note in Fig. 3 that inside of 3 Å, the NaH molecule with the additional two electrons provides greater deshielding at ^{39}Ar than does the bare Na$^+$ ion.

TABLE I. ^{39}Ar nuclear shielding $[\sigma(R)-\sigma(\infty)]$ as a function of ArNa distance and the dipole moment of the isolated NaH molecule.

R(Ar–Na), Å			$[\sigma(R)-\sigma(\infty)]$		
μ_{NaH} D	6.4498	6.7155	μ_{eq}=6.9898	7.2727	7.5637
2.0	−34.59	−32.86	−31.41	−30.32	−29.43
2.1	−30.09	−28.59	−27.40	−26.45	−25.67
2.3	−22.47	−21.29	−20.37	−19.63	−19.03
2.6	−13.46	−12.7	−12.10	−11.62	−11.25
2.9	−7.56	−7.21	−6.86	−6.58	−6.38
3.05		−5.40	−5.13	−4.94	−4.80
3.2	−4.3	−4.04	−3.85	−3.71	−3.61
3.5	−2.39	−2.26	−2.16	−2.10	−2.05
4.0	−0.98	−0.94	−0.92	−0.90	−0.90
5.0	−0.43	−0.43	−0.44	−0.44	−0.45

The R dependence of the *ab initio* shielding functions in the long-range limit for a rare gas atom in the presence of a neighbor is thoroughly consistent with the mean field model. Electric field gradient terms may be important for intermolecular shielding in molecular systems but they play no role in the isotropic average shielding of a rare gas atom in a medium. Finally, the charge distribution at the neighboring molecule or atom has a profound effect on the intermolecular shielding function.

IV. SCALING OF THE SHIELDING FUNCTIONS

Now that we have seen the general shapes and have related the long-range tails to the appropriate limiting forms at large R, let us consider how the magnitudes of various shielding functions are related to each other. There are several indications that scaling of the shielding functions might be possible. One is that the R dependence of the intermolecular shielding in various rare gas pairs appear to be nearly the same. For the range of R values greater than that corresponding to the minimum in the shielding function, the $\log[\sigma(\infty)-\sigma(R)]$/ppm vs $\log(R/\text{Å})$ plots reveal that ^{39}Ar in Ar···Ar, ^{39}Ar in Ar···Ne, ^{21}Ne in Ne···Ne, and ^{21}Ne in Ne···He have $\sim R^{-6.67}$, $\sim R^{-6.79}$, $\sim R^{-6.74}$, and $\sim R^{-7.41}$ dependences, respectively. We have proposed and found both theoretical and experimental support for the following scaling factors. First, there is the scaling which is suggested by the mean square electric field at position 1 due to mutually induced dipoles at atoms 1 and 2 as given by the London expression $\frac{3}{2}\alpha_2[U_1U_2/(U_1+U_2)]R^{-6}$. This suggests a scaling factor of the form $\sigma_2 U_1U_2/(U_1+U_2)$ in comparing one 1–2 pair with another 1–2′ pair of rare gases in the relevant range of R values sampled by $\exp[-V(R)/kT]$ at 200–400 K. We see that this approximation holds reasonably well in the ^{39}Ar shielding in the systems ArNe and ArAr in Fig. 4.

In this figure the R axis has been scaled by r_0 [the separation at which $V(R)=0$] for the rare gas pair potential function. The rationale for this is that the rare gas potential functions are very nearly conformal with scaled parameters ε and r_0. Although the shapes of $\sigma(R)$ are

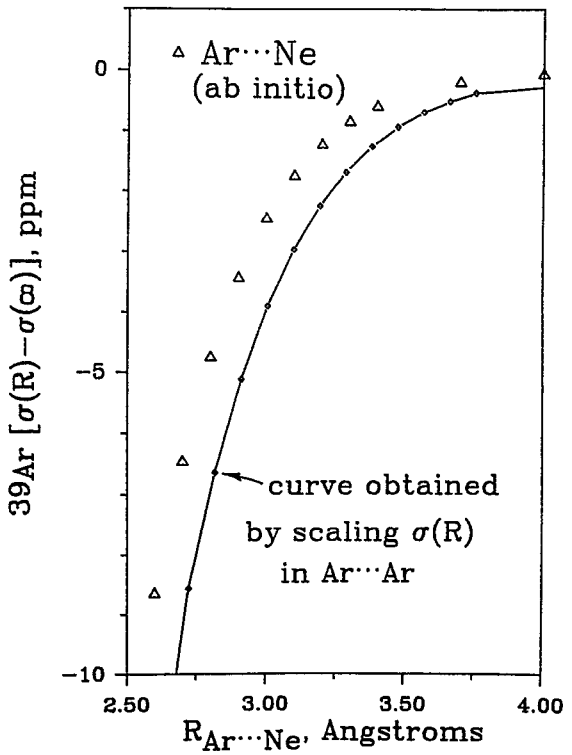

FIG. 4. The *ab initio* ^{39}Ar shielding surfaces for Ar···Ne and for Ar···Ar, scaled by the factor $\alpha_2 U_1 U_2/(U_1+U_2)$.

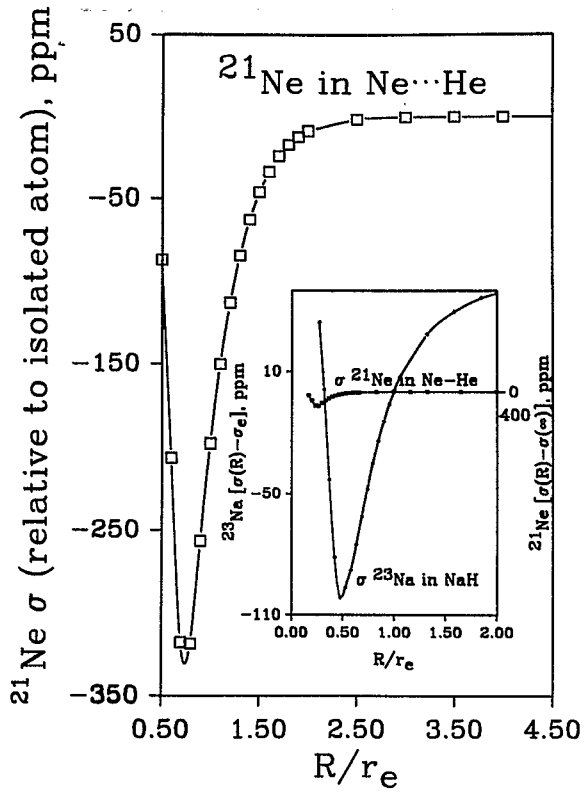

FIG. 5. The ^{21}Ne intermolecular shielding in Ne···He is compared with the ^{23}Na shielding in the isoelectronic diatomic molecule, NaH. The vertical scales are related by the values $\langle a_0^3/r^3\rangle_{np}$ in the Ne and Na atoms as a measure of the shielding sensitivity.

clearly reasonably close, the scaling along the R axis is not ideal.

Another scaling can be applied when the shielding of different nuclei are compared to each other. This is crucial to our interpretation of ^{129}Xe shielding, which we are unable to directly calculate at present. The factor $\langle a_0^3/r^3\rangle \cdot \alpha$ for the atom bearing the NMR nucleus was suggested in Ref. 12 as a scaling factor for what is effectively the quadratic response of the shielding to an electric field, $\frac{1}{3}\{\frac{1}{2}\alpha^{(2)}_{zz,z,z}+\sigma^{(2)}_{zz,x,x}\}$. The polarizability α provides the response of the electron distribution of the atom to the electric field and the $\langle a_0^3/r^3\rangle$ factor provides a measure of the sensitivity of the shielding to any changes in the electron distribution. The gross sensitivity of different nuclei to changes in electronic distribution in going from one molecule to another is reflected by the ranges in NMR chemical shifts. The periodic behavior of the experimental ranges in chemical shifts of nuclei has been shown to agree reasonably well with the periodic behavior of the $\langle a_0^3/r^3\rangle_{np}$ values obtained from the spin orbit splittings of the corresponding free atoms.[31] Thus the sensitivity of the shielding of a nucleus (in comparison with other nuclei) to changes in electronic environment is reflected by the value of $\langle a_0^3/r^3\rangle_{np}$. Altogether, the scaling factor we proposed is $[\langle a_0^3/r^3\rangle_{np}\cdot\alpha(0)]_1\alpha_2(0)U_1U_2/(U_1+U_2)$. The *ab initio* ^{39}Ar shielding in the Ar···Ar system scaled down to Ne···Ne compares very favorably with the *ab initio* ^{21}Ne shielding values in Ne···Ne for the range of values $R/r_{\min}>0.70$.[12] In fact, in the region $\sim 0.8r_0 < R < r_{\min}$ where exchange and overlap effects dominate the $[\sigma(R)-\sigma$ (free atom)] function, the scale factors convert all four *ab initio* shielding functions (for ^{39}Ar in Ar···Ar, and Ar···Ne and the ^{21}Ne shielding functions in Ne···Ne and Ne···He) into reasonably good facsimiles of each other. Furthermore, the scaling factors convert the ^{39}Ar in Ar_2 shielding function to approximate functions for ^{129}Xe shielding that reproduce fairly well the magnitudes and the temperature dependences of the experimental second virial coefficients of ^{129}Xe nuclear shielding in the XeAr, XeKr, and XeXe systems that have been in the literature for many years,[32] without the use of any adjustable parameters.[12]

Incidentally, we can apply the $\langle a_0^3/r^3\rangle$ scaling for a comparison of the shielding of ^{23}Na in the NaH molecule with the shielding of ^{21}Ne in the isoelectronic intermolecular system NeHe. In Fig. 5 we choose to scale the R axis to R_e, since this is the relevant characteristic distance in the NaH diatomic molecule. The object of this comparison is to note the relative magnitudes of the shielding changes accompanying the changes in intramolecular geometry as opposed to changes in intermolecular separation. Since these two are not observed in the same nucleus, the *ab initio* shielding surfaces are scaled by the factor $\langle a_0^3/r^3\rangle_{np}$ to put both nuclear shieldings on the same footing. That is, the vertical scales in Fig. 5 are related to each other by the ratio $\langle a_0^3/r^3\rangle_{np}$ for the Na and Ne atoms. This is again based on the well-established empirical relation between the periodic behavior of ranges of chemical shifts

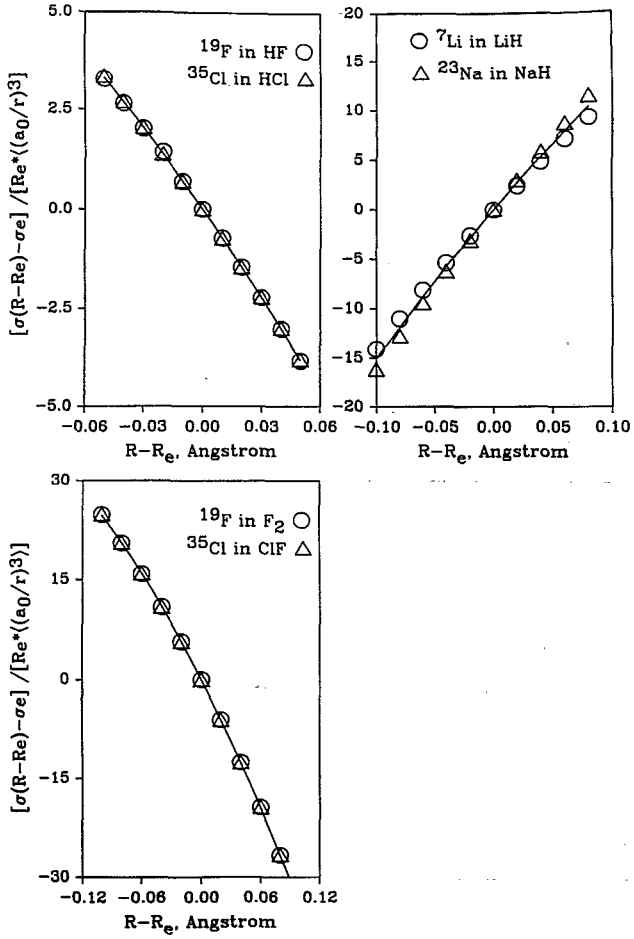

FIG. 6. The shielding surfaces of nuclei in analogous diatomic molecules in the vicinity of the equilibrium geometry, in the range of nuclear displacements spanning the classical turning points of the ground vibrational state. The equilibrium bond lengths are 1.4223 and 1.628 Å for F_2 and ClF (Refs. 33,34), 0.9169 and 1.2746 Å for FH and ClH (Refs. 35,36), and 1.594 and 1.889 Å for LiH and NaH (Refs. 35,37).

and of $\langle a_0^3/r^3\rangle_{np}$ for the free atom. Figure 5 provides the not surprising result that the magnitudes of shielding changes due to intermolecular interactions are considerably smaller than the shielding changes upon modification of intramolecular separations.

In a further study of the possible scaling of two-atom shielding functions, we examined the shapes of the shielding surfaces of diatomic molecules in the vicinity of the equilibrium geometry. These calculations were carried out using LORG and 6–311G basis sets with three added polarization functions of *d* type. Whereas the intermolecular shielding function in the range $R \approx 0.7r_0$ to $3\text{–}4r_0$ was found to scale by the factor $\langle a_0^3/r^3\rangle \cdot \alpha$ of the atom bearing the NMR nucleus, the change in shielding in diatomic molecules relative to the shielding at the equilibrium geometry appears to scale by the factor $\langle a_0^3/r^3\rangle \cdot R_e$ in the range of nuclear displacements spanning the classical turning points in the ground vibrational state. To show this, we compare in Fig. 6 different magnetic nuclei bonded to the same kind of atom, for systems in which the nuclei are related in the Periodic Table, so that the diatomic molecules are analogs. We do not yet fully understand the scaling by the factor R_e, but we suspect that the R_e scaling of $[\sigma(R)-\sigma(R_e)]$ is telling us something profound about the relationship between the electron distribution (as seen by the magnetic nucleus) and the equilibrium geometry. This may be analogous to the Herschbach–Lawrie general parametrized form of second, third, and fourth derivatives of $U(R)$ for diatomic molecules, all of which depend on R_e.[38] However, the profound connection, if there is one, escapes us at the present time. These comparisons are possible only for analogs and should be done with caution. Nevertheless, the superposability of the curves for different nuclei in Fig. 6 is quite impressive and the observed scaling again reinforces the similarities in the nature of the general shape of the shielding function.

V. THE RELEVANT REGION OF CONFIGURATION SPACE AND THE SIGN OF THE DERIVATIVE ($d\sigma/dR$) IN THAT REGION

The shielding that is observed experimentally depends on the relevant region of the shielding surface over which the averaging takes place. In Fig. 7 we attempt to show the relationships between the portion of the $\sigma(R)$ function that is of importance, and the potential energy function $V(R)$ which governs the averaging over the appropriate range of R values. The unit of energy in each subfigure is Kelvin, to indicate which portion of the potential function becomes relevant in the sampling of $\sigma(R)$ at any given temperature. The progression of the "active" range of R values across the $\sigma(R)$ function in going from ^{1}H in the H_2^+ molecule, to ^{23}Na in the NaH molecule, to ^{39}Ar in $ArNa^+$ and in Ar_2, provides different samplings of generally the same shape of $\sigma(R)$ function.

Although we cannot calculate the entire shielding function for nuclei in most diatomic molecules (for reasons stated earlier), we believe that they *all* nevertheless have shapes similar to those shown in Fig. 7 (excluding contributions from orbital paramagnetism in non-*S* systems). We offer as evidence the variation of the sign of the derivative of the shielding at R_e, $(d\sigma/dR)_{eq}$, among the hydrides of the first two rows of the periodic table. The change in sign was first noted by Chesnut.[3] For both first- and second-row hydrides, the shielding derivative starts out to be positive and small at the alkali end of the periodic table. A slight increase in the shielding derivative is observed upon going to the hydrides of the alkaline earth metals. Then a decrease in the derivative is observed upon going to boron and aluminum hydrides. This drop in the shielding derivative continues on, such that at the halogen end of the periodic table, it is generally negative and large. An explanation for this periodic trend has been proposed by Ditchfield[10] and, also, by Chesnut.[3] The difference in sign as observed between hydrogen halides and alkali hydrides was attributed to the change in the direction of polarization as dictated by the electronegativity of the heavy atom in the hydride. Our explanation for these trends suggests itself when the equilibrium bond lengths in these hy-

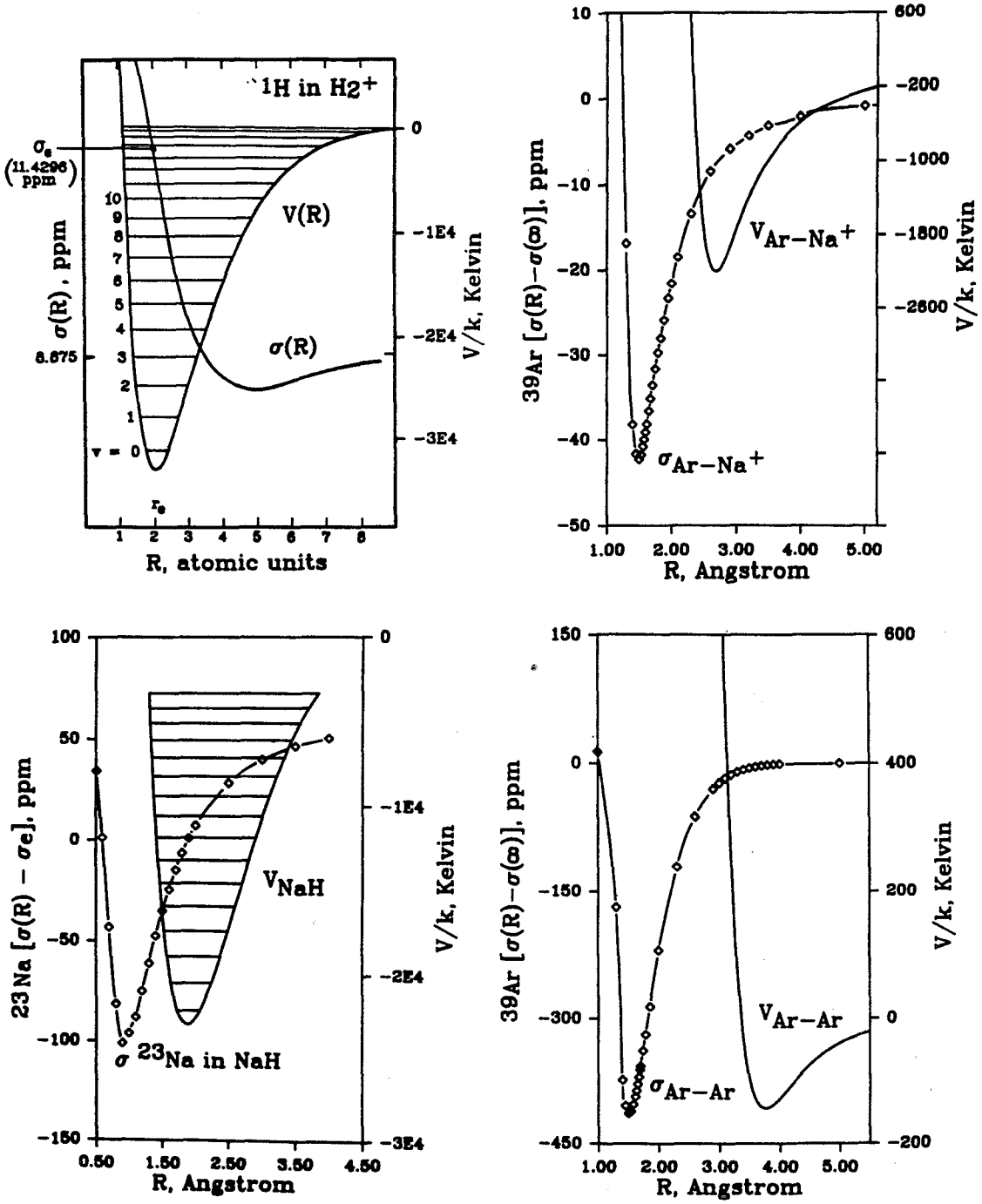

FIG. 7. The shielding surfaces, inter- and intramolecular, have qualitatively similar shapes. Potential functions are from Wind (Ref. 39) (H_2^+), Giroud and Nedelec (Ref. 37) (NaH), Viehland (Ref. 40) ($ArNa^+$), and Aziz and Chen (Ref. 41) (Ar_2). The shielding surfaces are from Hegstrom (Ref. 11) (H_2^+), Ref. 12, and this work.

drides are compared. In Fig. 8 we plot the shielding derivatives $(d\sigma^X/dR)_{eq}$ vs the equilibrium X–H bond length. The similarity between *inter*molecular and *intra*molecular shielding functions is clearly depicted in Fig. 8 by the similarity between the derivative function $d\sigma/dR$ vs R for ^{39}Ar in Ar_2 (for example) and the $(d\sigma/dR)_{eq}$ vs R_e for various hydrides.

The variation in sign of $(\partial\sigma^X/\partial R)_{eq}$ in the hydrides of rows 1 and 2 of the Periodic Table had been puzzling until now. With the assumption that the distance dependence of the shielding function has a universal shape, our interpretation of Fig. 8 is that glimpses into selected regions of this functional form are provided by the $(\partial\sigma^X/\partial R)$ values at the various equilibrium geometries of the XH_n hydrides. In going across the Periodic Table from LiH to FH and also from NaH to ClH, the derivatives $(\partial\sigma^X/\partial R)_{eq}$ trace out a functional form of $\sigma(R)$ which closely resembles the $(d\sigma/dR)$ function for ^{39}Ar in Ar_2 of the $(d\sigma/dR)$ function for

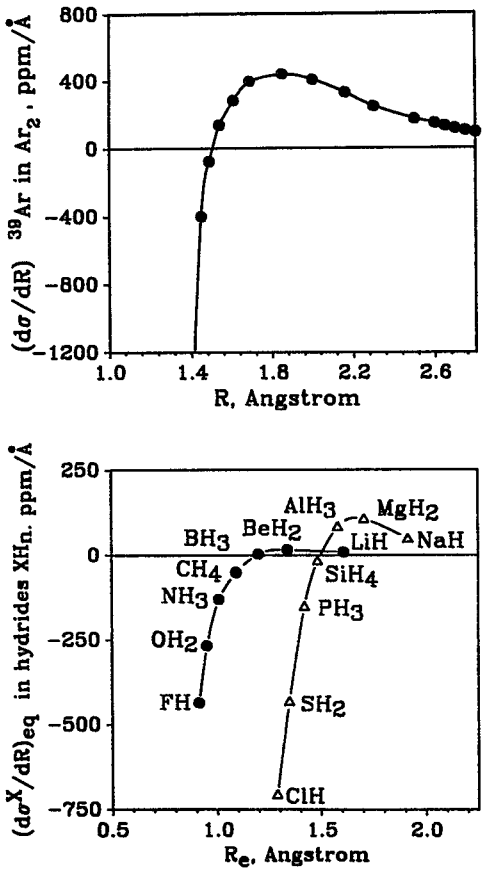

FIG. 8. Derivatives of the X nuclear shielding in XH_n (from Ref. 3) vary with R_e in the same way as the ^{39}Ar shielding derivative function in Ar···Ar.

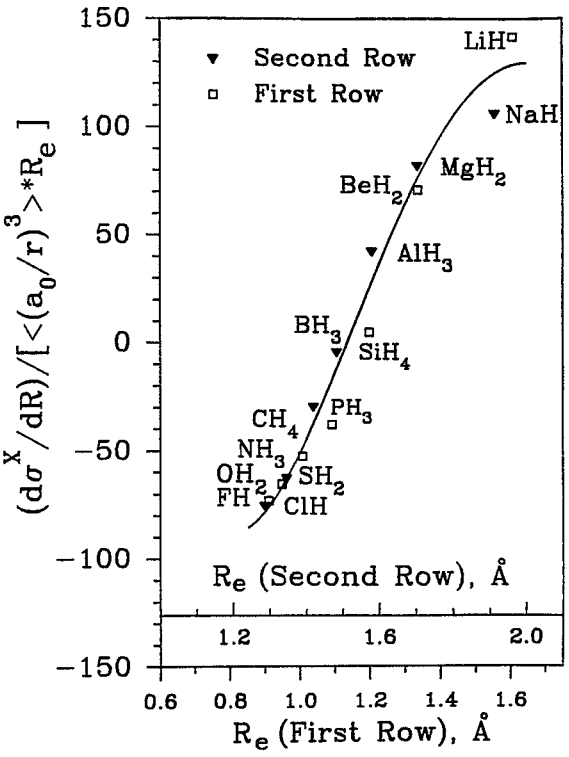

FIG. 9. Derivatives of the X nuclear shielding in XH_n (from Ref. 3) scaled by the scaling factors found in Fig. 6.

^{23}Na in NaH. Thus the way in which the $(\partial\sigma^X/\partial R)_{eq}$ varies across the Periodic Table for XH_n hydrides now appears entirely normal and comprehensible.

In one final comparison, the scaling of the $\sigma(R)$ functions observed in Fig. 6 can be combined with Fig. 8 to see the general shape of the shielding surface. If indeed, the empirical scaling factors found in Fig. 6 can be used to relate shielding surfaces of different nuclei, one should be able to perceive the conformity of shielding surfaces by a comparison of the shielding derivatives, scaled by $[\langle a_0^3/r^3\rangle \cdot R_e]$ across the Periodic Table. Both the first and second row hydrides are displayed in Fig. 9. The shape is indeed very similar to that which we found for the $(d\sigma/dR)$ function calculated from Hegstrom's $\sigma(R)$ surface[11] for ^1H in H_2^+.

VI. CONCLUSIONS

We report *ab initio* calculations of nuclear shielding over a wide range of internuclear separations in the following systems for the first time: ^{23}Na in the NaH molecule, ^{39}Ar in ArNe, ^{21}Ne in NeHe, and ^{39}Ar in Ar···NaH (collinear). We offer a possibly universal shape of the shielding function for any two-atom system. We provide a rationale for the types of *ab initio* numerical functional forms found in the large R region in the various systems studied here (and also including the previously reported shielding functions for ^{39}Ar in Ar_2 and $ArNa^+$) by using the shielding hyperpolarizabilities and the long-range limiting analytic forms associated with the latter in connection with electrical moments of the interacting species.

We have also calculated nuclear shieldings in the range of nuclear displacements spanning the classical turning points of the ground vibrational states for ^{35}Cl in ClF, ^{19}F in F_2, ^{35}Cl in ClH, ^{19}F in FH, ^{23}Na in NaH and ^7Li in LiH. With the assumption of a universal shape of the shielding function of nucleus X with respect to internuclear separation in all the hydrides XH_n of the first and second row of the Periodic Table, we provide an interpretation of the variation, across the Periodic Table, of shielding derivatives $(\partial\sigma^X/\partial R)_{eq}$ at the equilibrium geometries of these hydrides. We view these derivatives as glimpses into various different short segments of the shielding function, with the segment selection varying smoothly across the Periodic Table as the nature of the chemical bond dictates the value of the equilibrium bond length for the hydride. By discovering the scaling factors that relate shielding functions of different nuclei, we bring out a conformity of σ^X of all first and second row hydrides, and in so doing, we believe that we have traced out the functional R dependence of all of them. With this work, the shielding function, intermolecular and intramolecular, for a two-atom system has been placed in a framework that allows the similarities between them to be evident and allows a unified picture to emerge.

Furthermore, in discovering empirical scaling factors (containing only atomic or molecular constants and no adjustable parameters) that relate shielding functions of different nuclei, the magnitudes and signs of the changes in shielding with geometry in different systems can be related to each other.

ACKNOWLEDGMENT

This research has been supported by the National Science Foundation (Grant No. CHE92-10790).

[1] C. J. Jameson, Chem. Rev. **91**, 1375 (1991).
[2] C. J. Jameson and H.-J. Osten, Ann. Rept. NMR Spectrosc. **17**, 1 (1986).
[3] D. B. Chesnut, Chem. Phys. **110**, 415 (1986).
[4] D. B. Chesnut and D. W. Wright, J. Comput. Chem. **12**, 546 (1991).
[5] D. B. Chesnut and C. K. Foley, J. Chem. Phys. **84**, 852 (1986).
[6] P. W. Fowler, G. Riley, and W. T. Raynes, Mol. Phys. **42**, 1463 (1981).
[7] P. Lazzeretti, R. Zanasi, A. J. Sadlej, and W. T. Raynes, Mol. Phys. **62**, 605 (1987).
[8] C. J. Jameson, A. C. de Dios, and A. K. Jameson, J. Chem. Phys. **95**, 9042 (1991).
[9] C. J. Jameson, A. C. de Dios, and A. K. Jameson, J. Chem. Phys. **95**, 1069 (1991).
[10] R. Ditchfield, Chem. Phys. **63**, 185 (1981).
[11] R. A. Hegstrom, Phys. Rev. A **19**, 17 (1979).
[12] C. J. Jameson and A. C. de Dios, J. Chem. Phys. **97**, 417 (1992).
[13] C. J. Jameson, J. Chem. Phys. **66**, 4977 (1977).
[14] A. E. Hansen and T. D. Bouman, J. Chem. Phys. **82**, 5035 (1985).
[15] T. D. Bouman and A. E. Hansen, Chem. Phys. Lett. **175**, 292 (1990).
[16] GAUSSIAN 88, M. J. Frisch, M. Head-Gordon, H. B. Schlegel, K. Raghavachari, J. S. Binkley, C. Gonzalez, D. J. Fox, R. A. Whiteside, R. Seeger, C. F. Melius, J. Baker, R. Martin, L. R. Kahn, J. J. P. Stewart, E. M. Fluder, S. Topial, and J. A. Pople (Gaussian, Inc., Pittsburgh, 1988).
[17] RPAC version 8.5, Thomas D. Bouman, Southern Illinois University at Edwardsville, and Aage E. Hansen, H. C. Oersted Institute, Denmark.
[18] A. D. Buckingham, Can. J. Chem. **38**, 300 (1960).
[19] T. W. Marshall and J. A. Pople, Mol. Phys. **1**, 199 (1958).
[20] W. T. Raynes and R. Ratcliffe, Mol. Phys. **37**, 571 (1979).
[21] J. D. Augspurger, C. E. Dykstra, and E. Oldfield, J. Am. Chem. Soc. **113**, 2447 (1991).
[22] J. D. Augspurger and C. E. Dykstra, J. Phys. Chem. **95**, 9230 (1991).
[23] A. D. Buckingham, Adv. Chem. Phys. **12**, 107 (1967).
[24] J. I. Musher, Adv. Magn. Reson. **2**, 177 (1962).
[25] F. London, Z. Phys. Chem. (Leipzig) B **11**, 222 (1930).
[26] F. London, Trans. Faraday Soc. **33**, 8 (1937).
[27] A. D. Buckingham and K. L. Clarke, Chem. Phys. Lett. **57**, 321 (1978).
[28] A. D. Buckingham and K. P. Lawley, Mol. Phys. **3**, 219 (1960).
[29] R. S. Mulliken, Phys. Rev. **50**, 1028 (1936).
[30] W. T. Raynes, A. D. Buckingham, and H. J. Bernstein, J. Chem. Phys. **36**, 3481 (1962).
[31] C. J. Jameson and J. Mason, *Multinuclear NMR*, edited by J. Mason (Plenum, New York, 1987), pp. 51–88.
[32] C. J. Jameson, A. K. Jameson, and S. M. Cohen, J. Chem. Phys. **62**, 4224 (1975).
[33] W. Stricker and J. C. Hochenbleicher, Z. Naturforsch. Teil A **28**, 27 (1973).
[34] R. E. Willis Jr., Ph.D. thesis, Duke University, 1979.
[35] G. Herzberg, *Spectra of Diatomic Molecules* (Van Nostrand, Princeton, 1950).
[36] J. K. G. Watson, J. Mol. Spectrosc. **45**, 99 (1973).
[37] M. Giroud and O. Nedelec, J. Chem. Phys. **73**, 4151 (1980).
[38] D. R. Herschbach and V. W. Laurie, J. Chem. Phys. **35**, 458 (1961).
[39] H. Wind, J. Chem. Phys. **42**, 2371 (1965); **43**, 2956 (1965).
[40] L. A. Viehland, Chem. Phys. **85**, 291 (1984).
[41] R. A. Aziz and H. H. Chen, J. Chem. Phys. **67**, 5719 (1977).